Radio Science, Volume ???, Number , Pages 1–19,

Coherent Subtraction of Narrowband Radio Frequency Interference

Kyehun Lee

Electrical and Computer Engineering, Virginia Polytechnic Institute and State University, Blacksburg, Virginia, USA

Steven W. Ellingson

Electrical and Computer Engineering, Virginia Polytechnic Institute and State University, Blacksburg, Virginia, USA

K. Lee, Mobile and Portable Radio Research Group 432 Durham Hall, Mail Stop 0350 Bradley Department of Electrical and Computer Engineering Virginia Polytechnic Institute and State University Blacksburg, VA 24061, USA (kylee1@vt.edu)

Abstract: The ability to do radio astronomy at wavelengths $>$ 1 m is frequently restricted by narrowband anthropogenic radio frequency interference (RFI). Much new science requires observations at frequencies where RFI can not be avoided. There have been attempts to suppress RFI using signal processing techniques, with performance which is found to be limited by the interference–to–noise ratio (INR). This paper describes a generic suppression method applicable to all narrowband RFI signals, as well as a method which is particularly effective against narrowband frequency modulated (NBFM) signals. Both methods are based on a strategy of estimation followed by coherent subtraction, and neither requires an additional reference antenna. The generic method is shown to be somewhat "toxic" to underlying noise and astronomical signals but may nevertheless have applications; whereas the NBFM–specific method is shown to be relatively benign to astronomical signals but also somewhat less effective in suppressing RFI. The performance of both methods is demonstrated with a real–world data consisting of 4 narrowband FM signals.

1. Introduction

Anthropogenic radio frequency interference (RFI) poses severe challenges for radio astronomy [*Thompson et al.,* 1991]. Whereas it is often possible to employ a strategy of avoidance – e.g., observing in bands which are protected by regulation, or from sites at which RFI is acceptably weak – much important science requires observations at sites and in bands in which RFI cannot be effectively avoided. For example, a topic which is currently of intense interest to the astronomical community is the possibility of studying the Epoch of Reionization using the redshifted 21 cm emission of hydrogen (e.g., [*Furlanetto et al.,* 2004]), and is a prime motivator for a number of new radio telescopes currently under construction including the Low Frequency Array (LOFAR) [*Butcher,* 2004], the Mileura Widefield Array (MWA) [MWA website], and the Square Kilometer Array (SKA) [SKA website]. This effort requires access to large contiguous segments of quiet spectrum ranging from ∼75 MHz to ∼250 MHz. For a variety of reasons the new instruments LOFAR and the Long Wavelength Array (LWA) [LWA website] intend to operate at frequencies as low as 20 MHz.

Although many forms of RFI exist in the range 20–250 MHz, a common and particularly onerous source is "narrowband" (3 kHz to 25 kHz bandwidth) voice communications using various amplitude, phase, and frequency modulation techniques. This category of signals can be found nearly everywhere, both because they are frequently used for mobile communications including aircraft, and because signals at these frequencies can propagate over extraordinary distances. These aspects limit the extent

to which a strategy of avoidance can be successful, and motivate technical solutions in which RFI-afflicted data might instead be cleaned, preferably in real time.

Although extensive literature exists on the problem of mitigation of RFI (e.g., [*Laster and Reed*, 1997] and references therein) the vast majority of past work is oriented toward communication applications, as opposed to radio science applications. The resulting emphasis is on the reduction of very strong RFI – i.e., interference-to-noise ratios (INR) orders of magnitude greater than 1. RFI whose INR is less than or equal to 1 is typically no longer limiting to communication performance. In radio science applications, in contrast, input INR ≤ 1 can be devastating; e.g., in spectroscopy involving long integrations. Thus, we seek algorithms which are effective in suppressing weak RFI to INR $\ll 1$. Additionally, we seek algorithms which do this without distorting the underlying astronomy and, preferably, also not distorting the underlying noise.

Notable previous attempts to mitigate narrowband RFI in a manner germane to radio astronomy includes [*Barnbaum and Bradley,* 1998], which addressed the feasibility of using a time-domain adaptive canceler in this application. This approach requires an auxiliary signal which has nominally a high-INR copy of the RFI and negligible SNR for the astronomical signal of interest, and must therefore be obtained from a separate "reference" antenna. Thus limitations of this approach are that (1) some *a priori* information about the location of the signal is required so as to properly point the reference antenna(s), and (2) the technique is limited to suppression which is proportional to the INR achieved in the reference channel. We refer to the

principle that this class of mitigation techniques tends to produce output INR equal to the inverse of the input INR as "power inversion". Power inversion tends to limit the usefulness of affected algorithms since RFI which appears weak over short time–frames can easily ruin observations made over longer time periods. In the Bradley and Barnbaum approach, the only alternative is to increase the gain of the reference antenna.

An interesting alternative approach can be found in the synthetic aperture radar literature [*Miller et al.,* 1997], in which the RFI is modeled as sinusoids of unknown frequency, magnitude, and phase. The proposed algorithm then consists of dynamically estimating these parameters, synthesizing new (noise-free) versions of the signals using the estimated parameters, and then coherently subtracting these from the original data. This technique turns out to be highly effective especially when the sample rate is much greater than the Nyquist criterion for any given RFI signal, since in this case, narrowband RFI signals are well-modeled as unmodulated carriers, even over large numbers of samples. Furthermore, there is no need for a separate reference antenna. To accommodate frequency–modulated signals having bandwidth too great to model effectively as sinusoids, this approach adds an additional parameter – the first derivative of frequency with respect to time – which in effect extends the signal model to include "linear chirp" signals. The disadvantage of this approach is that the algorithm has no means to distinguish between RFI and noise, and thus tends to suppress both. This can be problematic for the detection of weak signals underlying the RFI. Ironically, the performance of this approach is also constrained by the

power inversion principle; in fact severely so since, in the basic algorithm, there is no reference antenna to increase the input INR. Detailed discussion of this issue can be found in [*Ellingson*, 2002]. [*Ellingson and Hampson*, 2003] describes a specific application of the sinusoidal estimation and subtraction approach to L-band astronomy afflicted by ground based aviation radar, where the limitations of both power inversion and detection sensitivity are observed. Although one might consider some combination of the above two approaches to overcome this difficulty; that is, using a reference antenna to increase the input INR and thereby improving the estimation of sinusoidal parameters, in the present work we wish to avoid the implementation problems associated with a reference antenna.

[*Ellingson et al.*, 2001] addressed this difficulty by employing *a priori* information about the modulation of the RFI signal to improve the "effective" INR of the received RFI. They demonstrate more than 20 dB of suppression of a GLONASS (direct sequence spread spectrum satellite) signal received at an INR of -20 dB; i.e., suppression at least 20 dB greater than that implied by the power inversion constraint. In this case, the fact that the modulated bandwidth is orders of magnitude greater than the message (pre-modulation) signal – i.e., large "processing gain" – is exploited to convert the problem from that of estimating the parameters of the rapidly-changing modulated RF waveform with low INR to that of estimating the parameters of the slowly-varying message waveform with high INR. In terms of implementation, this turns out to be a simple matter of demodulating the signal to retrieve the information

signal, and then remodulating the signal to obtain a noise-free version of the original signal.

In this paper, we attempt to extend this "modulation-savvy" approach to improve the performance of RFI mitigation following the parametric estimation and subtraction strategy of [*Miller et al.,* 1997]. Specifically, we exploit the significant (but relatively modest) processing gain and "constant modulus" (magnitude) properties of narrowband FM (NBFM) signals to achieve the benefits of this approach with reduced distortion of the underlying signals of interest.

This paper is organized as follows. Section 2 presents a RFI signal model and its characteristics, the background theory of the suggested RFI mitigation method, and design parameters appropriate for mitigation of RFI of interest. In Section 3, we demonstrate the performance of the mitigation method with real–world data. Section 4 provides concluding remarks including recommendations for further improvement.

2. Theory

In this paper, we model the signal received by a radio telescope as

$$x(t) = \sum_{n=1}^{N} s_n(t) + s_a(t) + z(t) \tag{1}$$

where $z(t)$ is additive white Gaussian noise, $s_a(t)$ is an astronomical signal of interest, and $s_n(t)$ are RFI signals having the form:

$$s_n(t) = a_n(t)e^{j\{\omega_n(t)t+\theta_n(t)\}} \tag{2}$$

The meanings and behaviors of the parameters in (2) depend on the modulation of the RFI signal. For amplitude-modulated signals including single-sideband (SSB), $a_n(t)$ is the audio "message" signal; $\omega_n(t)$ is the carrier frequency which varies only slightly and slowly due to a combination of the limited frequency stability of transmitting equipment and Doppler effects; and $\theta_n(t)$ is an arbitrary phase offset which also varies very slowly, primarily in response to propagation conditions. The parameters result in occupied bandwidth of less than 5 kHz, which is only slightly larger than the typical message bandwidth of 3 kHz.

For NBFM signals, the message is represented by $\theta_n(t)$, and $a_n(t)$ varies only slightly and slowly, relative to the inverse message bandwidth, due primarily to multipath fading [*Jakes*, 1974]. Because $a_n(t)$ is nominally constant, FM signals are said to have "constant modulus", a property we exploit in this paper. Standard bandwidths for NBFM signals are 25 kHz, 12.5 kHz, and (now rare but likely to become more common) 6.25 kHz [TIA, 2004]. The relatively large occupied bandwidth compared to the message bandwidth means NBFM signals contain a considerable degree of redundant information; this is essentially the "processing gain" referred to in Section 1. This processing gain is exploited in NBFM systems to achieve improved audio quality; however here we take advantage of it in much the same manner it is exploited in [*Ellingson et al.*, 2001]; that is, to bypass the power inversion constraint and to enhance discrimination between signal and noise.

The proposed algorithm is shown in Figure 1. It works by (1) finding the number of signals (i.e., "model order estimation") and making coarse estimates ω_n^c of their center

frequencies, (2) estimating parameters, a_n, ω_n, and θ_n, for each signal identified, (3) synthesizing estimates of the associated signals $s_n(t)$, and (4) subtracting these from a delayed version of $x(t)$, nominally yielding the desired signal $y(t) = s_a(t) + z(t)$. Important to note in Figure 1 is that the "primary path" includes delay to account for latency incurred in the estimation and synthesis of RFI signals in other paths. The latency of concern is dominated by the delay incurred in finite impulse response (FIR) filters, thus the primary path latency is deterministic and easily introduced in the form of an all-pass FIR filter of appropriate length.

Many possible methods exist for model order estimation and coarse frequency estimation [*Stoica and Moses*, 2005]. In our work, this is conveniently implemented using a fast fourier transform (FFT). The length of the FFT, T_{FFT}, is chosen so as to yield a resolution bandwidth small enough to clearly resolve adjacent signals. The update rate T_1 for the estimates of model order and coarse frequency can be orders of magnitude greater than T_{FFT}, and thus the sensitivity of detection can be increased by using the smallest possible T_{FFT} and averaging the resulting spectra over T_1. The criteria for detection is based on a threshold test. The value of the threshold β is most conveniently expressed in units of standard deviations (σ) of the noise, $z(t)$, distribution above the mean of $z(t)$, and the selected value is chosen as a tradeoff between good sensitivity (tending to relatively low β) and low "false alarm" rate (tending to relatively high β). The specific danger in having an excessive false alarm rate is that the misguided attempts to estimate and subtract non-existent signals

will result in increased distortion of $z(t)$ and possibly also $s_a(t)$. In practice, β in the range 5σ to 10σ is known to be effective [*Ellingson and Hampson*, 2003].

Figure 2 shows a generic estimation procedure which is applicable to all narrowband modulations. In this procedure, RFI signal of interest is first isolated using a bandpass filter (BPF) centered at ω_n^c. Then, the parameters, a_n, ω_n, and θ_n, are estimated by assuming that RFI is sinusoidal over the period of T_2 since the last update of the parameters. With ω_n^c from coarse frequency search, the procedure is to find ω_n which maximizes the magnitude of (3) given by

$$A = \frac{1}{T_2}\int_0^{T_2} x_n(t)e^{-j\omega_n t}dt \tag{3}$$

This is conveniently done as a binary search over the bandwidth of the BPF, starting at ω_n^c. For ω_n maximizing (3), A becomes

$$A = a_n e^{j\theta_n} \tag{4}$$

Then, a_n, ω_n, and θ_n are the optimal Maximum Likelihood estimates.

The precise implementation of the generic estimation procedure should be optimized to the type of signal being processed. The bandpass filter should be wide enough to include the entire bandwidth of the RFI signal, plus any error in the initial coarse frequency estimate; reasonable values are 5 kHz for SSB and 15 kHz for NBFM. The update rate T_2 for sinusoidal parameter estimation is a tradeoff between sensitivity (favoring relatively long T_2) and desire to accurately track parameter variations resulting from modulation (favoring relatively short T_2). In practice, T_2 should be approximately one-tenth of the inverse bandwidth of the signal; i.e., 20 μs for SSB

and 6.7 μs for NBFM. To avoid jitter resulting from endpoint effects in the estimation of parameters, it is recommended to apply a Bartlett (triangular) window over the time-domain samples to be processed to obtain any given update.

Figure 3 shows an improved procedure which is applicable to NBFM signals. In this case, $x_n(t)$ is demodulated by computing the time-derivative of $\theta_n(t)$, which yields the message signal. This is then low-pass filtered to suppress extraneous noise. The processing gain is obtained by the fact that the message signal is mostly preserved, whereas any noise outside the low-pass bandwidth is suppressed. The message signal is then remodulated by time-domain integration and addition of initial phase offset to obtain the improved estimate of θ_n. Concerning LPF design, the passband must include the entire message spectrum, and passband ripple must be minimized to prevent error in the remodulated signal. Note that the principal advantage in this procedure is that the new sinusoidal phase estimates now respond primarily to the signal *alone*, as opposed to the combination of signal plus noise. Thus, this procedure reduces the extent to which the algorithm distorts $s_a(t)+z(t)$, as will be demonstrated in the next section.

A second modification for the NBFM-specific procedure of Figure 3 is that the constant modulus property of NBFM is exploited to improve the estimation of a_n. This is achieved by averaging the estimates over a period T_3 which is as long as possible, but much shorter than the "channel coherence time" which is the time over which the gain associated with propagation channel can be assumed to be relatively constant. The channel coherence time is approximately given by $T_C \approx 0.423/f_{Dm}$

where f_{Dm} is the maximum Doppler shift [*Rappaport,* 1996]. In the experiment shown in Section 3, for example, the carrier frequency is ∼162 MHz. Therefore, assuming the RFI transmitter is moving with the speed of 30 m/s, T_C becomes 26 ms; thus a reasonable value for T_3 is 3.9 ms, i.e, much shorter than T_C and much longer than noise correlation distance induced by the BPF. It should be noted that the advantage obtained by enforcing constant modulus is similar to that obtained using the "demod-remod" technique to improve θ_n; that is, that estimates now respond primarily to the signal alone, as opposed to the combination of signal plus noise.

3. Experiment

To demonstrate the effectiveness of the proposed algorithm, we applied it to a real–world example of NBFM signals. The data consists of four separate weather radio stations operated by the U.S. National Oceanic and Atmospheric Administration located in Arizona (Southwest USA). This includes a station at 162.400 MHz located at Flagstaff, a station at 162.425 MHz located at Payson (Mt. Ord), a station at 162.500 MHz located at Globe (Signal Peak), and a station at 162.550 MHz located at Phoenix. The data provided to the algorithm is in complex baseband form sampled at 256 kSPS, and the total record to be evaluated is ∼1 seconds long. The average spectrum is shown in Figure 4. It can be seen that the modulation is of the 12.5 kHz variety, and that the INRs range from ∼0.7 dB to ∼24 dB within ∼200 kHz–wide passband. Note that the spectrum of each signal includes a strong narrow peak which seems to be independent of the expected modulation. The explanation for this

feature can be seen in Figure 5, which shows the dataset in the form of a spectrogram. The narrow peak corresponds to periods, visible in the spectrogram, over which the carrier is effectively unmodulated. These unmodulated periods occur because these stations continue to transmit even when there is no voice activity.

The algorithm parameters used to process this data are as follows: in model order detection and the coarse frequency search, T_{FFT} =2 ms, $\beta = 10\sigma$, and detection is done just once over the duration of the dataset ($T_1 \approx 1$ s).

First, we consider the results using the generic processing method of Figure 2 with $T_2 = 6.7$ μs. The result is shown in Figure 6. Note that the generic processing algorithm results in the deep suppression of all four NBFM signals. However, noise which occupies the same bandwidth as RFI signal is also suppressed. This is due to the algorithm's inability to discriminate RFI from noise.

Next, we consider the results using the NBFM-specific processing method of Figure 3 with $T_2 = 6.7$ μs and $T_3 = 3.9$ ms. The bandwidth of the LPF following the differentiator is set at 4 kHz, which includes the entire message spectrum. ω_n is estimated just once, i.e., $T_4 \sim 1$ s. The result is shown in Figure 7. Note in this case noise spectrum is preserved, but the RFI is not as deeply suppressed.

Finally, we consider the potential toxicity of the RFI processing to weak astronomical signals, $s_a(t)$. To do this, we created simulated spectral lines in the form of sinusoids added to the data, with two cases of frequency offset, 1 and 5 kHz, above the center frequency of each of the 4 RFI signals, and with magnitude such that it has SNR of $\sim$6 dB with respect to the resolution bandwidth of the spectrum shown in

Figure 1. The spectrum of these signals by themselves is shown in Figure 8 for 1 kHz offset. Figures 9–11 show the results for generic and NBFM-specific processing. In Figure 9, it can be seen that the generic processing method suppresses all signals, including the artificial spectral lines. Thus, the generic algorithm is not suitable for spectroscopy. In Figures 10 and 11, the suppression results with NBFM–specific processing are seen to depend on the frequency offsets. In case of 1 kHz offset, the simulated spectral lines are suppressed by $\sim$50%. In case of 5 kHz offset, they are preserved. The reason the lines with 5 kHz offset are preserved whereas the lines with 1 kHz offset are not is explained by the bandwidth of the LPF in the "demod–remod" path in Figure 3, which is 4 kHz in this example. Thus, the choice of the bandwidth of this LPF is a trade–off between a large value (e.g., 5 kHz), which provides the most effective suppression, and a small value (e.g., 3 kHz), which protects largest fraction of bandwidth against the toxic effect of the mitigation algorithm.

4. Concluding Remarks

This paper has described and demonstrated a method for mitigation for a broad class of narrowband signals which are common sources of interference to radio science observations in the range 20–250 MHz and beyond. The basic approach is to model RFI signals as sinusoids, and then to synthesize and subtract noise-free versions of these sinusoids from the original received signal. Two methods for estimating signal parameters were presented: A generic method which assumes only that RFI is well modeled as sinusoids, and a NBFM-specific method which exploits the constant

modulus property and significant processing gain inherent in NBFM signals to improve discrimination between RFI and noise. It was demonstrated that the former tends to distort components of the signal other than the RFI, whereas the latter is considerably better in this regard, but less effective in suppression the RFI.

We should note that the generic method, despite its tendency to "eat" noise and other signals underlying the RFI signals, is not completely without utility. For example, elimination of strong RFI – even if the underlying spectrum is rendered unusable – may nevertheless be desirable as it allows the data to be represented using a smaller number of bits, which may have compelling advantages in some systems. Although the same effect can be accomplished by, for example, computing spectra and then blanking (zeroing) RFI-afflicted bins, this method is entirely coherent and does not require transformation of the signal into the frequency domain, which might be problematic or impossible in some systems. Another possible application of the generic algorithm is pulsar processing, which is less sensitive to the observed "notching" behavior than spectroscopy.

It should be pointed out that while we have not explicitly quantified the computational complexity of the proposed algorithms, we emphasize that it is well within the capabilities of existing conventional off-the-shelf real-time digital signal processing. In fact, this processing is similar or identical to processing performed by the communications equipment associated with these signals; e.g., detection, demodulation, and so on. Because these are typically commercial/commodity products, there has

been considerable previous effort invested in identifying minimum cost/complexity implementations; see for example [*Vassilevsky, V.L.*, 2007].

Finally, we should note that the algorithms described in Section 2 are applicable to all forms of narrowband amplitude-, phase-, and frequency-modulated signals that can be described in terms of the signal model of equation (2). This includes CW (i.e., morse code), and the plethora of narrowband phase- and frequency-modulated digital signals that exist. Moreover, it should be noted that digital signals have the additional property of "finite alphabet" – that is, the parameters of the transmitted signal are constrained to take on only a countable number of values, in contrast to analog signals in which the parameters vary continuously. This is another form of *a priori* waveform knowledge that can be exploited for additional performance improvement. The possibility of exploiting the finite alphabet property of narrowband digital signals is not considered here but is addressed in the context of a wideband digital signal in [*Ellingson et al.*, 2001].

Conversely, we should point out that there are a number of RFI signals in the frequency range of interest for which the performance of the approach proposed here is relatively poor. Prominent among these are broadcast FM signals ranging from 88 to 108 MHz in the U.S., which are relatively wideband (bandwidths on the order of 200 kHz) and thus require update times (T_2) which are very short. In this case, the linear chirp approach used in [*Miller et al.,* 1997] might be helpful. In addition, broadcast FM signals contain additional structure including a pilot signal, subcarriers for stereo, radio broadcast data system (RBDS), and subsidiary communications

authorization (SCA). They must be taken into account to obtain the best performance. Performance will be limited for analog TV (NTSC) and digital TV (ATSC) for similar reasons. However, we note that there is no reason that the concepts described in this paper and in [*Ellingson et al.*, 2001] could not be combined and/or extended for these RFI signals.

Acknowledgments. The data used in Section 3 was provided by Michael Gray, who has made this and other datasets freely available via his website http://www.kd7lmo.net/ground_gnuradio_ota.html.

References

Barnbaum, C. and R. Bradley (1998), A New Approach to Interference Excision in Radio Astronomy: Real-Time Adaptive Cancellation, *Astronomical J.*, 115, 2598.

Butcher, Harvey R. (2004), LOFAR: first of a new generation of radio telescopes, *Proceedings of the SPIE*, 5489, 537.

Ellingson, S.W., J. Bunton, and J.F. Bell (2001), Removal of the GLONASS C/A Signal from OH Spectral Line Observations Using a Parametric Modeling Technique, *Astrophysical Journal Supplement*, 135, 87.

Ellingson, S.W. (2002), Capabilities and Limitations of Adaptive Canceling for Microwave Radiometry, IEEE 2002 Int'l Geoscience and Remote Sensing Symposium (IGARSS 2002), Toronto, 3, 1685.

Ellingson, S.W. and G.A. Hampson (2003), Mitigation of Radar Interference in L-Band Radio Astronomy, *Astrophysical Journal Supplement Series*, 147, 167.

Furlanetto, S.R., M. Zaldarriaga, and L. Hernquist (2004), Statistical Probes of Reionization with 21 Centimeter Tomography, *Astrophysical J.*, 613, 16.

Jakes, W. C. (1974), *Microwave Mobile Communications*, IEEE Press.

Laster, J. D. and J. H. Reed (1997), Interference Rejection in Digital Wireless Communications, *IEEE Signal Processing Magazine*, 14, 37.

Long Wavelength Array (LWA) website at http://lwa.unm.edu.

Miller, T. R., J. McCorkle, and L. C. Potter (1997), RFI suppression for ultra wideband radar, *IEEE Transactions on Aerospace and Electronic Systems*, 33, 1142.

Mileura Widefield Array (MWA) website at http://www.haystack.mit.edu/ast/arrays/mwa.

Rappaport, Theodore S. (1996), *Wireless Communications: Principles and Practice*, Prentice Hall PTR, Upper Saddle River, New Jersey.

Square Kilometer Array (SKA) website at http://www.skatelescope.org.

Stoica, P. and R. Moses (2005), *Spectral Analysis of Signals*, Pearson Prentice Hall, Upper Saddle River, New Jersey.

Thompson, A. R., Tomas E. Gergely and Paul A. Vanden Bout (1991), Interference and Radioastronomy, *Physics Today*, November, 41.

Telecommunications Industry Association (2004), TIA Standard: Land Mobile FM or PM - Communications Equipment - Measurement and Performance Standards, TIA-603-C.

Vassilevsky, V.L., (2007), Efficient Multitone Detection, *IEEE Signal Processing Mag.*, 24 (2), 144.

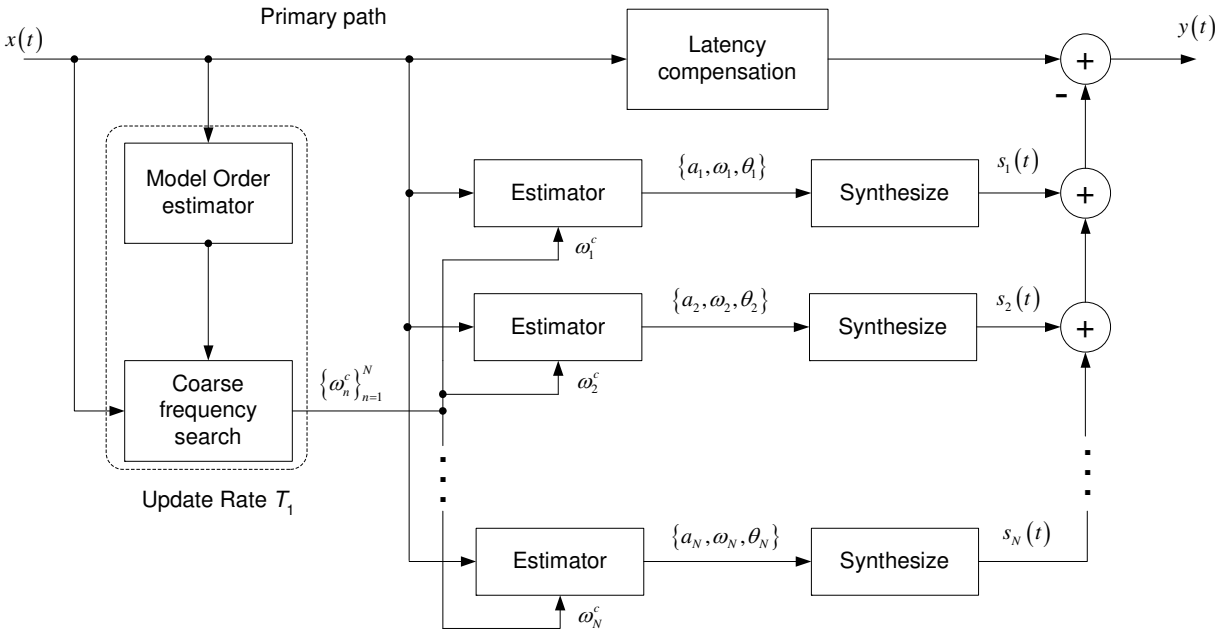

Figure 1. Top-level block diagram of the algorithm.

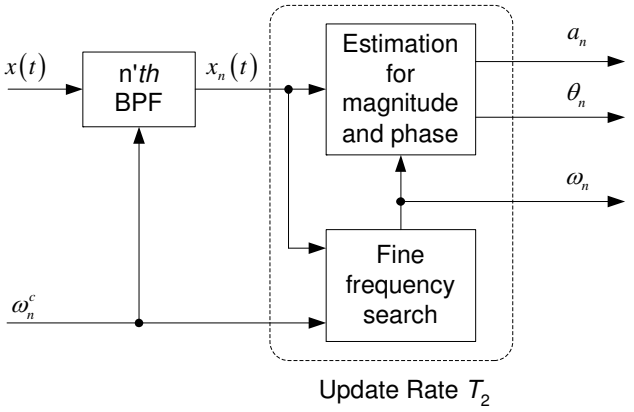

Figure 2. Detail of generic estimation procedure.

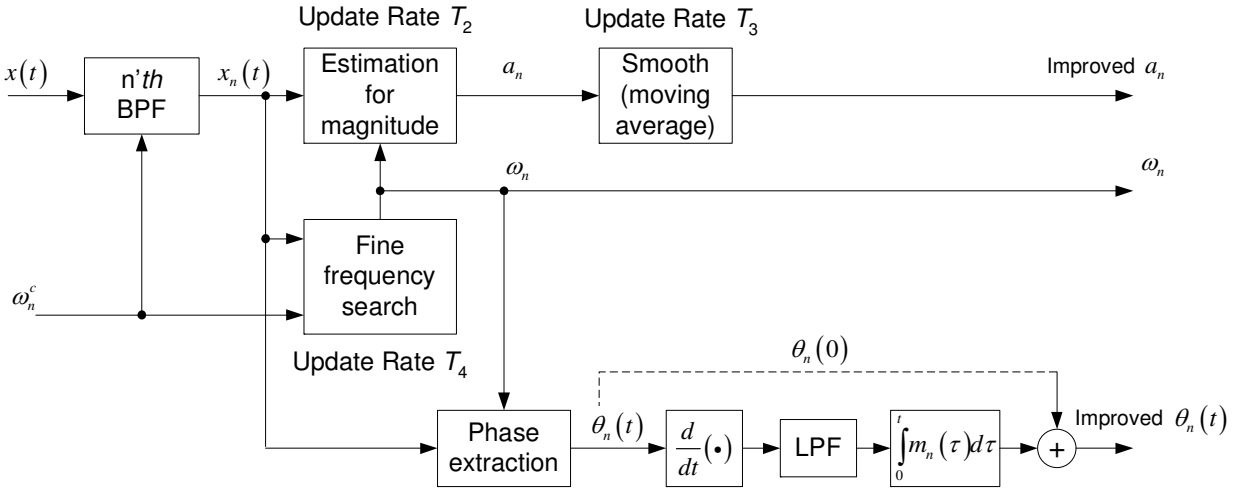

Figure 3. Detail of improved estimation procedure for NBFM signals.

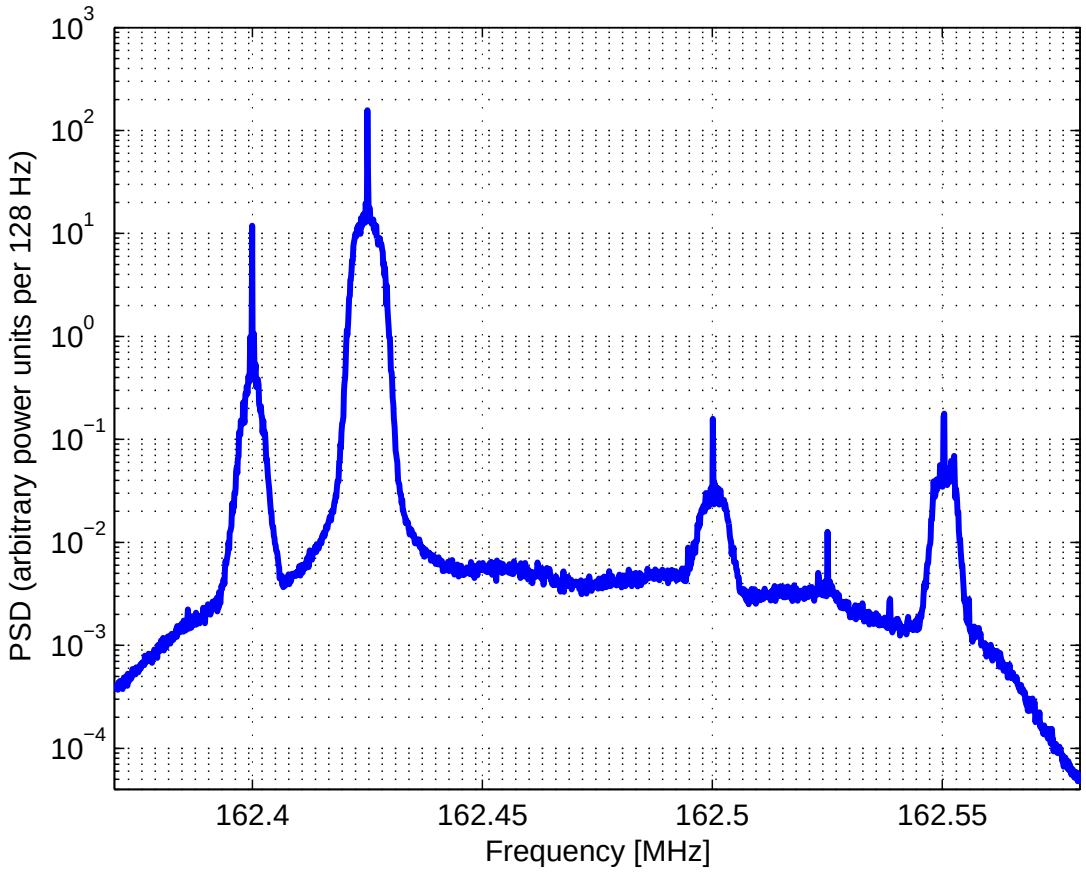

Figure 4. Power spectral density (PSD) of test dataset averaged over 0.967 s.

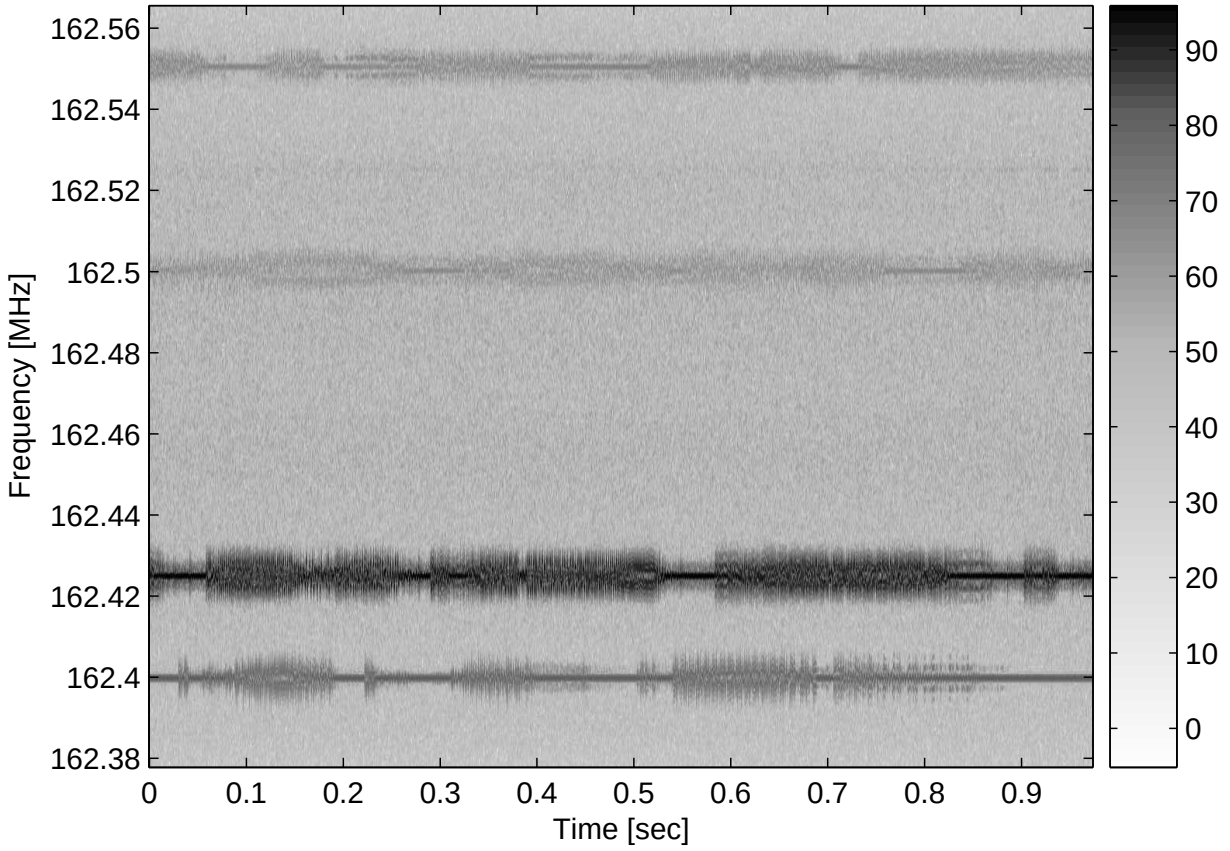

Figure 5. Spectrogram (power spectral density vs. time and frequency) for the dataset.

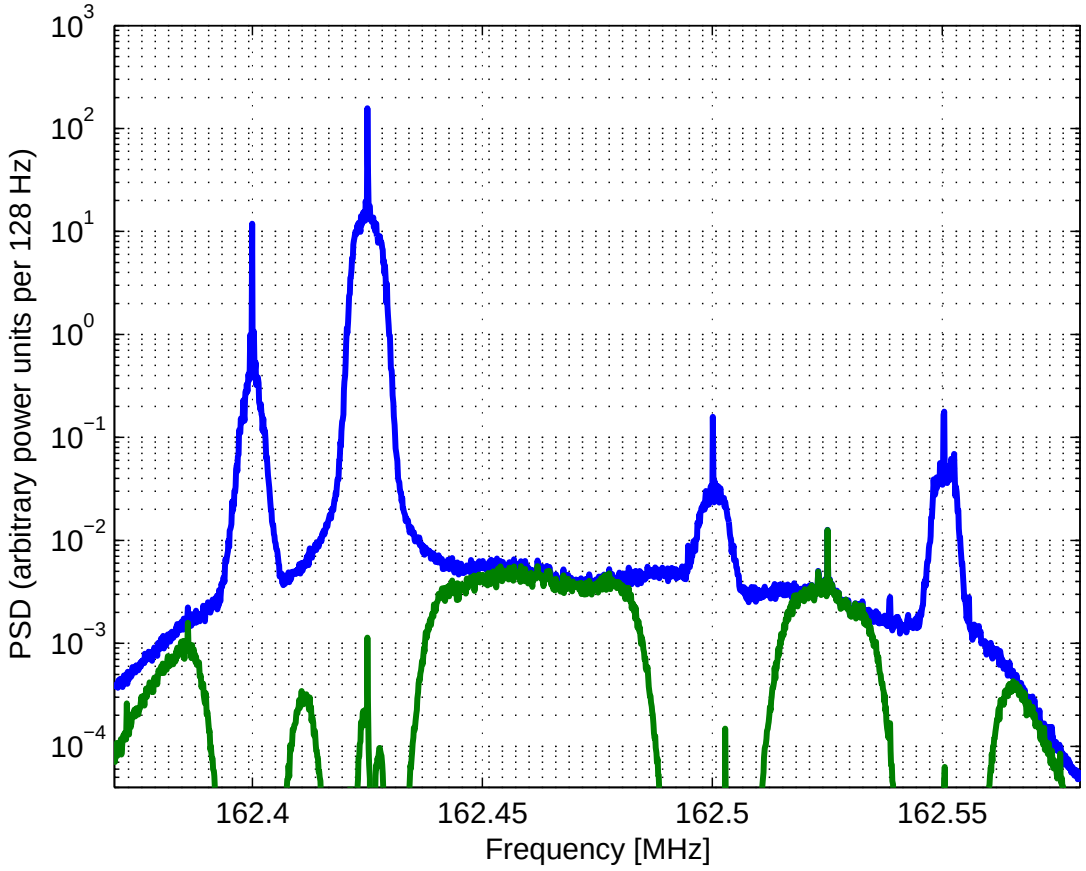

Figure 6. Averaged power spectral density before (top) and after (bottom) application of the generic mitigation algorithm (Figure 2).

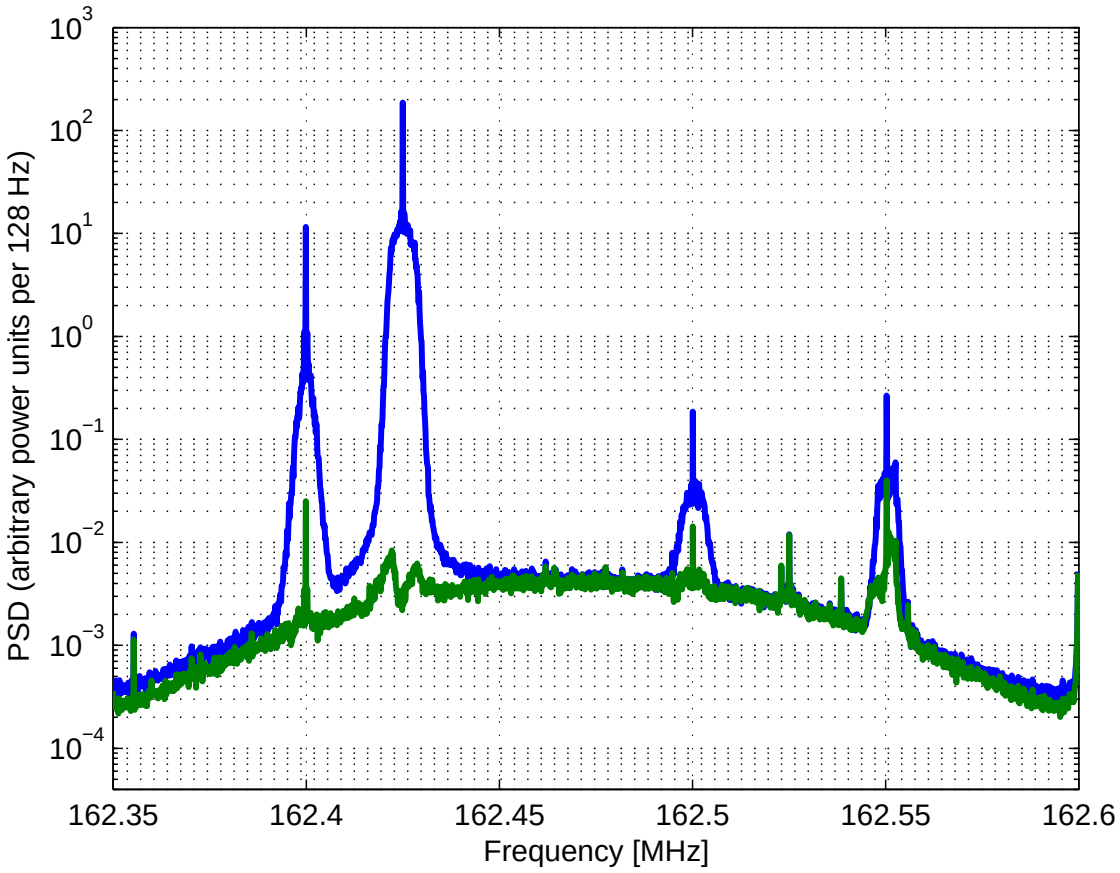

Figure 7. Averaged power spectral density before (top) and after (bottom) application of the NBFM–specific mitigation algorithm (Figure 3).

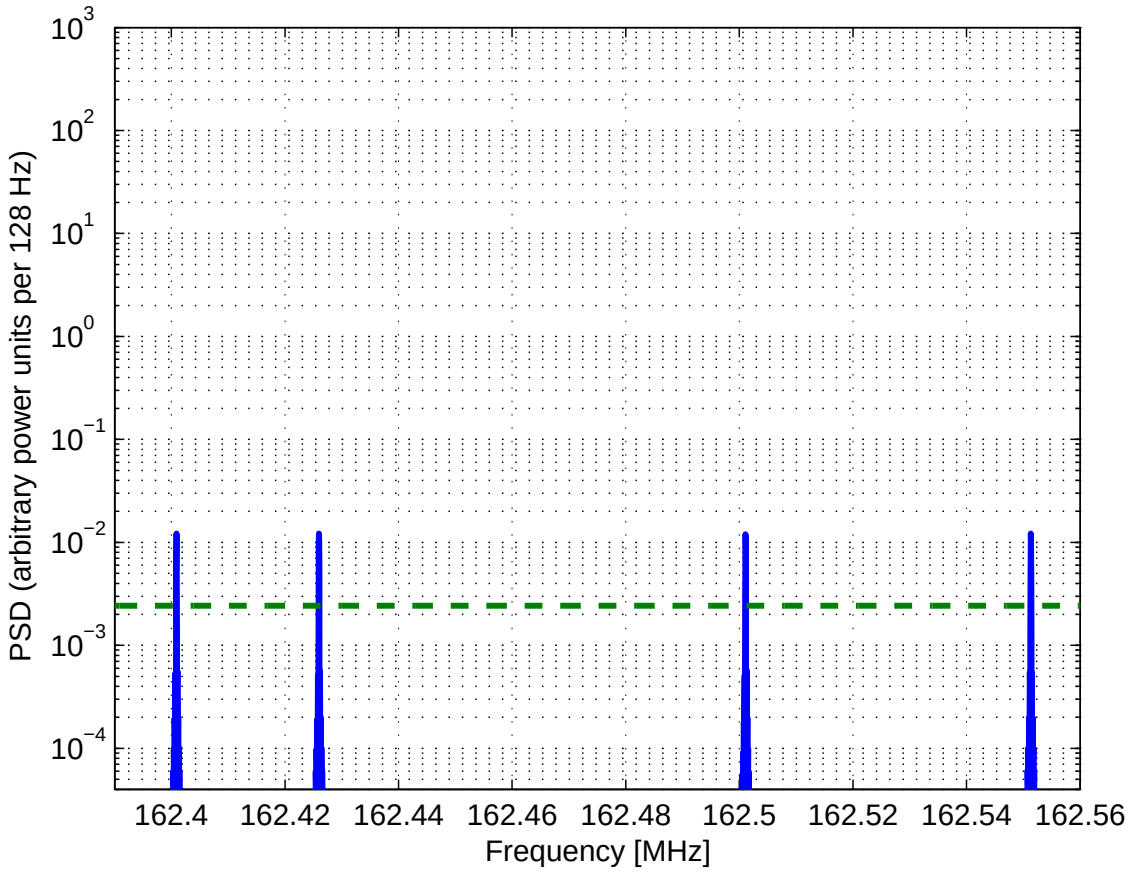

Figure 8. Averaged power spectral density of 4 sinusoids located at 1 kHz above the center frequencies of the RFI signals. The dash line is the mean of noise power spectral density.

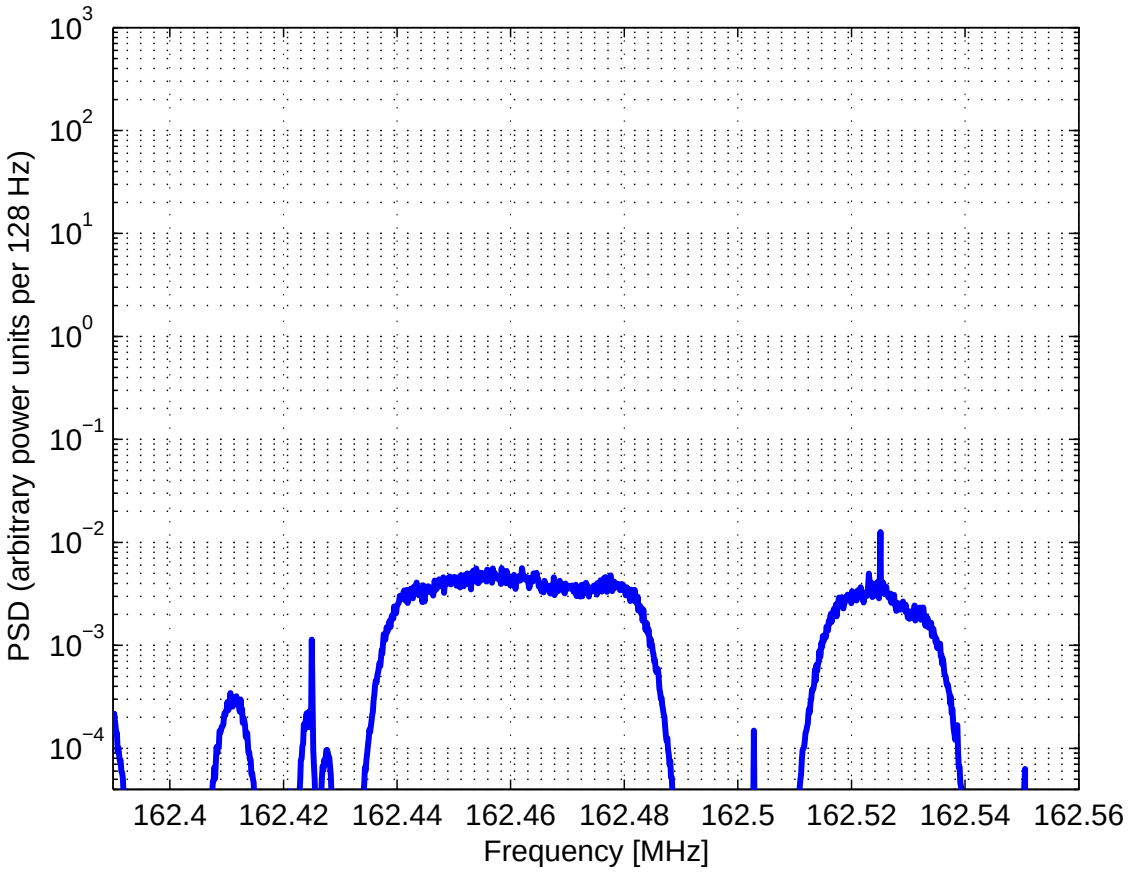

Figure 9. Averaged power spectral density after application of the generic mitigation algorithm (Figure 2) with 4 additional sinusoid signals at 1 kHz offset.

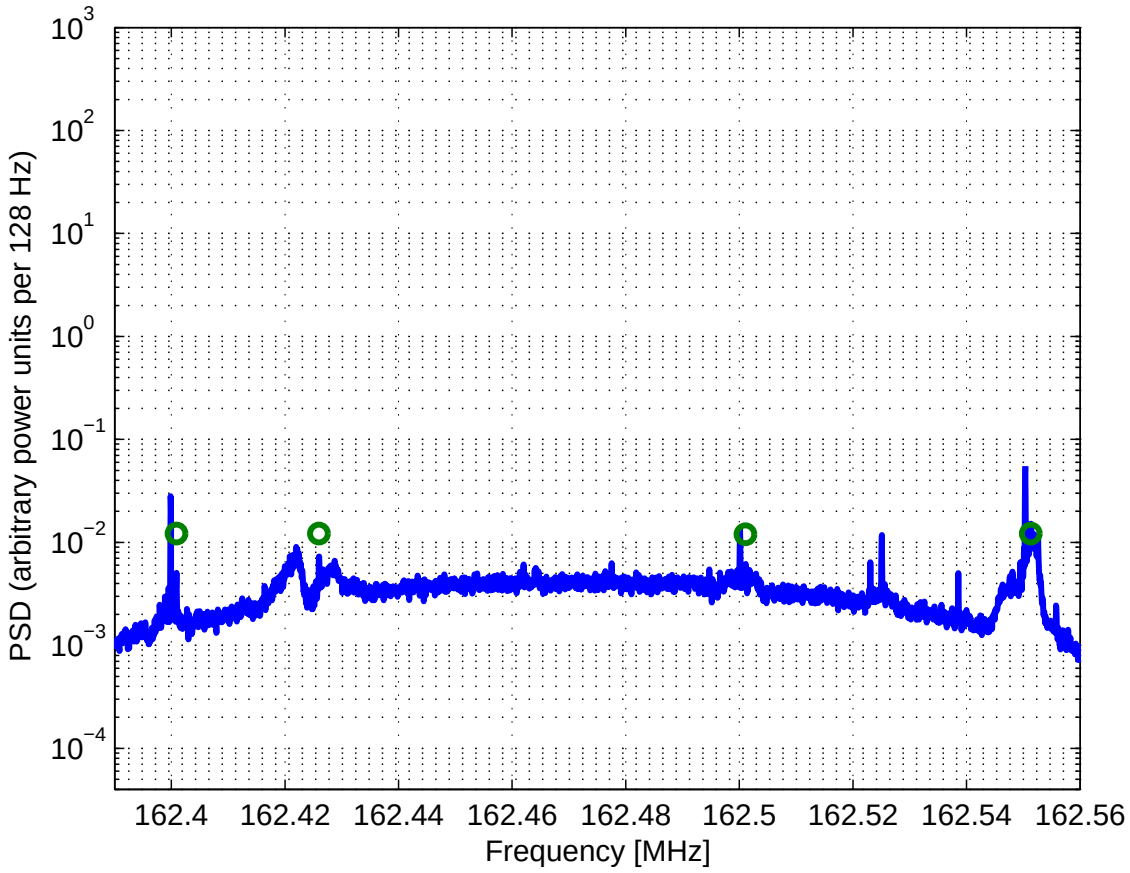

Figure 10. Averaged power spectral density after application of the NBFM–specific mitigation algorithm (Figure 3) with 4 additional sinusoid signals at 1 kHz offset. Markers indicate the proper frequency and level of the additional signals.

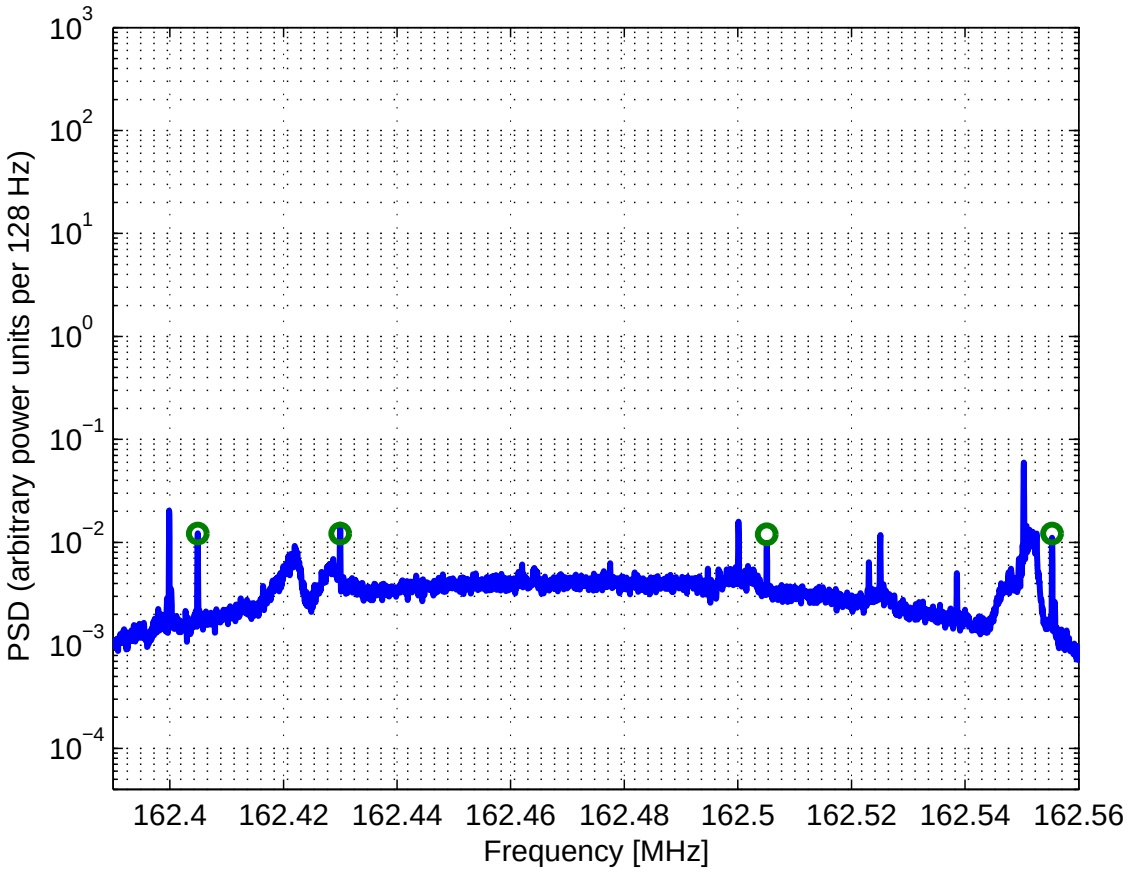

Figure 11. Averaged power spectral density after application of the NBFM–specific mitigation algorithm (Figure 3) with 4 additional sinusoid signals at 5 kHz offset. Markers indicate the proper frequency and level of the additional signals.